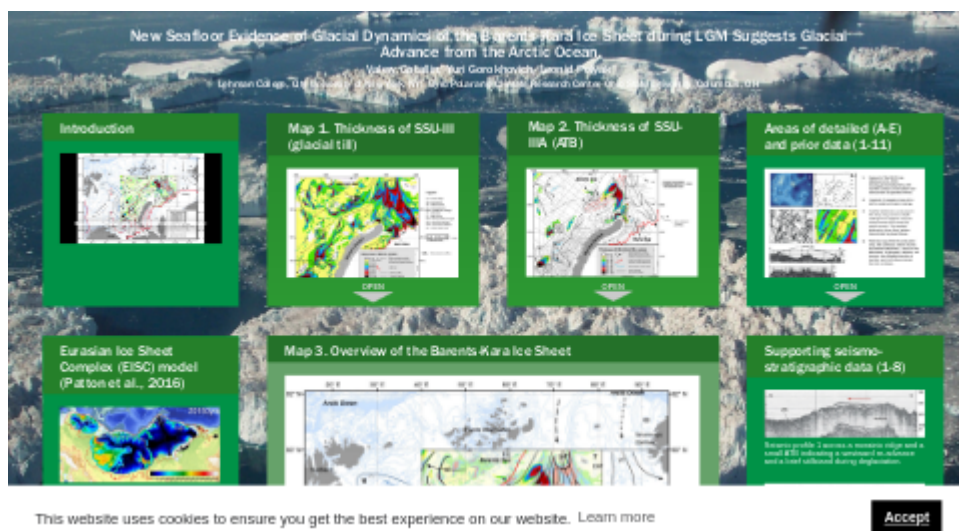


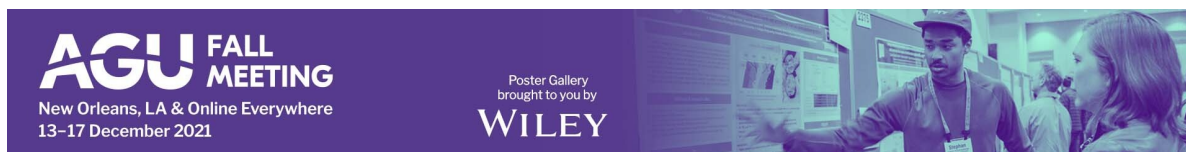
New Seafloor Evidence of Glacial Dynamics of the Barents-Kara Ice Sheet during LGM Suggests Glacial Advance from the Arctic Ocean



Valery Gatallin, Yuri Gorokhov, Leonid Polyak

Lehman College, City University of New York, NY; Byrd Polar and Climate Research Center, Ohio State University, Columbus, OH

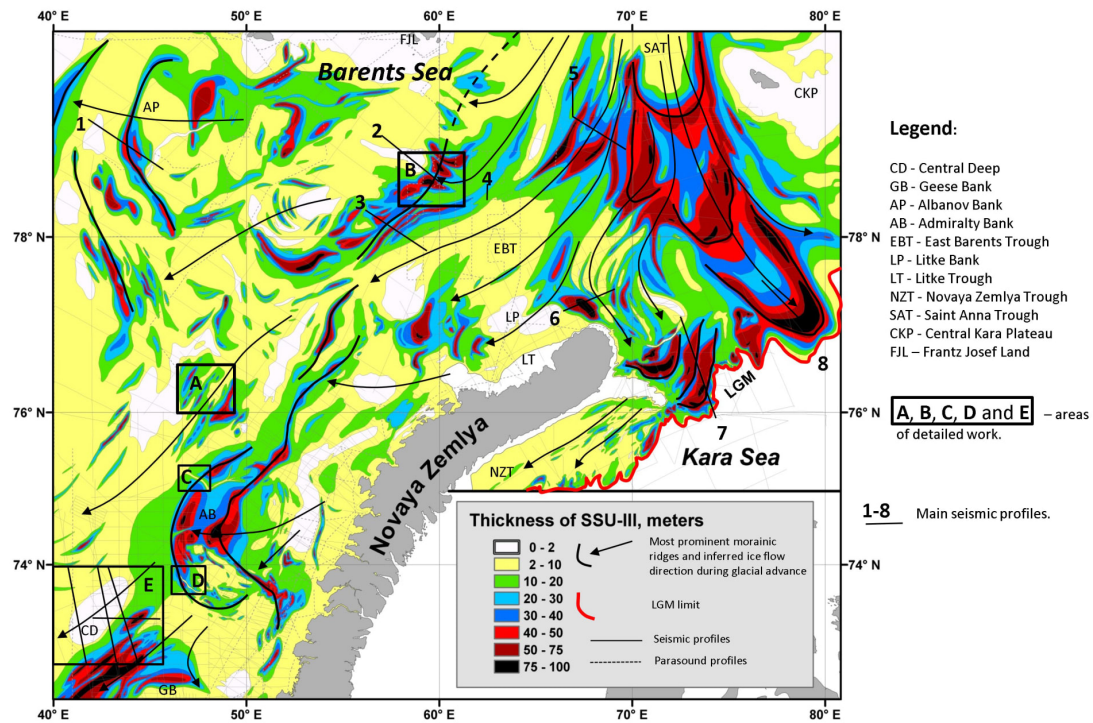
PRESENTED AT:



INTRODUCTION

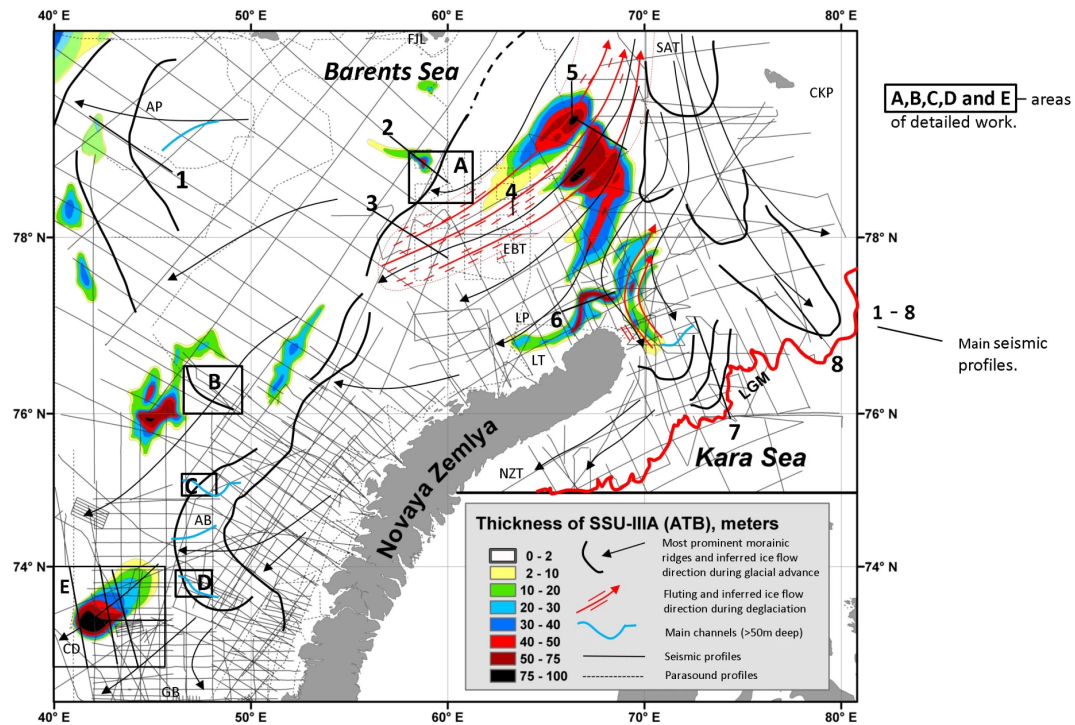
[VIDEO] https://res.cloudinary.com/amuze-interactive/video/upload/vc_auto/v1638451249/agu-fm2021/DE-4E-3F-2D-D0-69-7B-A0-6D-A3-A6-15-24-B2-83-84/Video/Sequence_01_hd_270_tdtjdj.mp4

MAP 1. THICKNESS OF SSU-III (GLACIAL TILL)



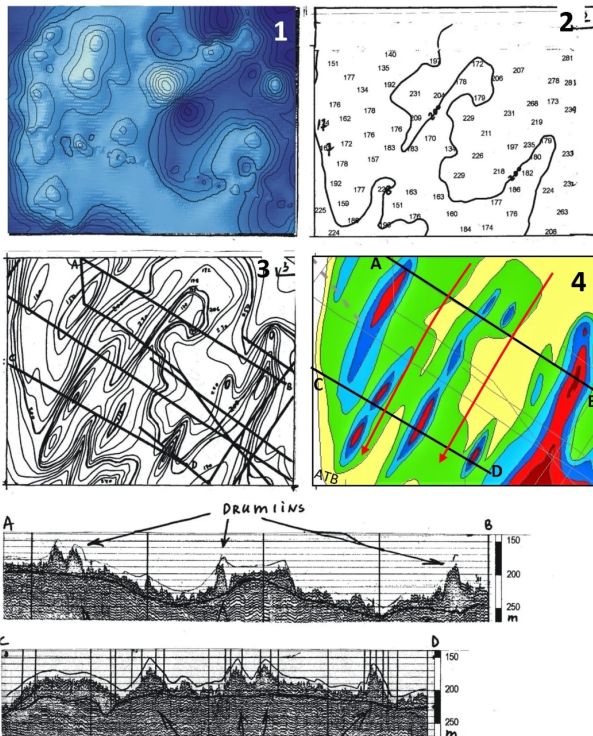
Thickness map of seismostratigraphic unit SSU-III (glacial till) showing a southward glacial advance via Saint Anna Trough (SAT).

MAP 2. THICKNESS OF SSU-IIIA (ATB)



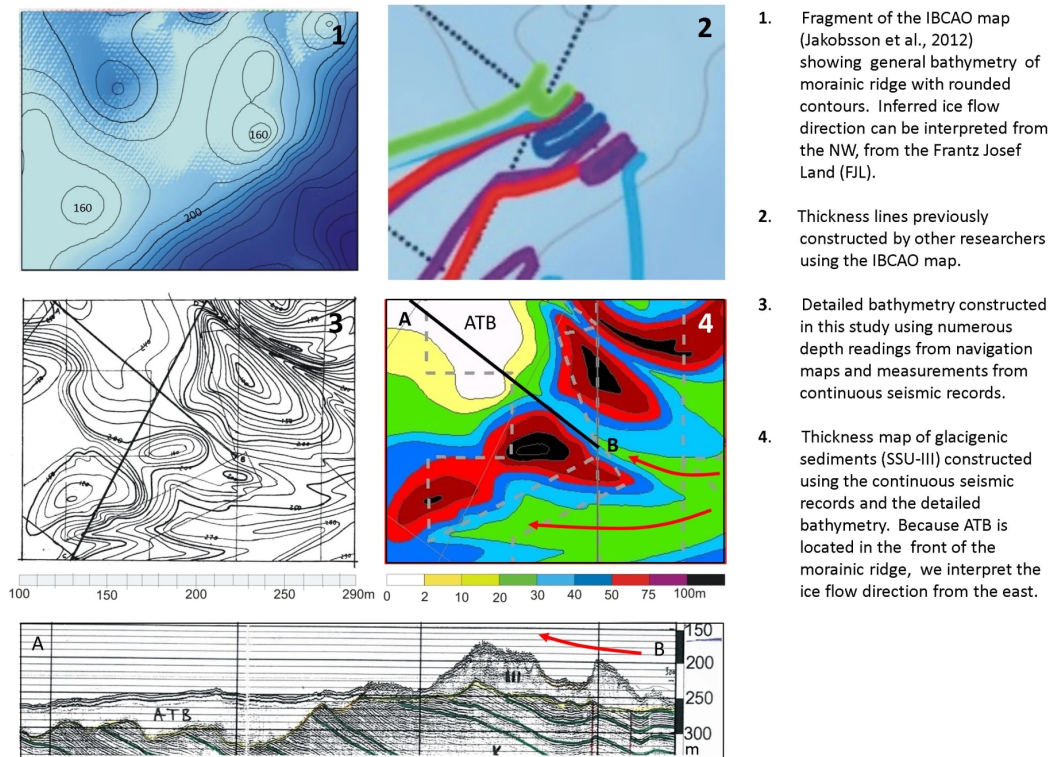
During deglaciation the ice flow reversed its direction towards the SAT (ice free by that time), forming lineated seafloor features in the East Barents Trough (EBT) and a massive Acoustically Transparent Body (ATB) on the western SAT slope.

AREAS OF DETAILED (A-E) AND PRIOR DATA (1-11)

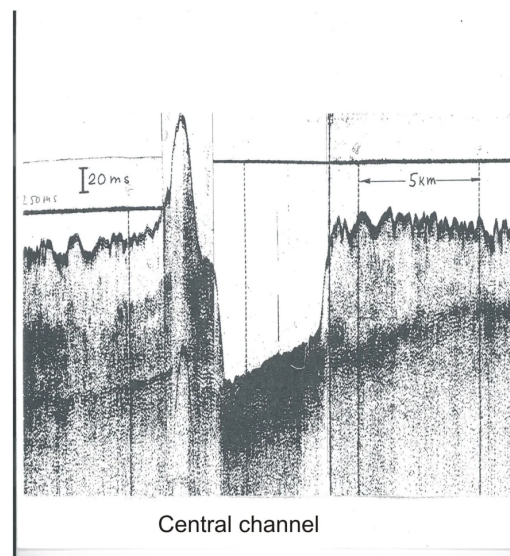
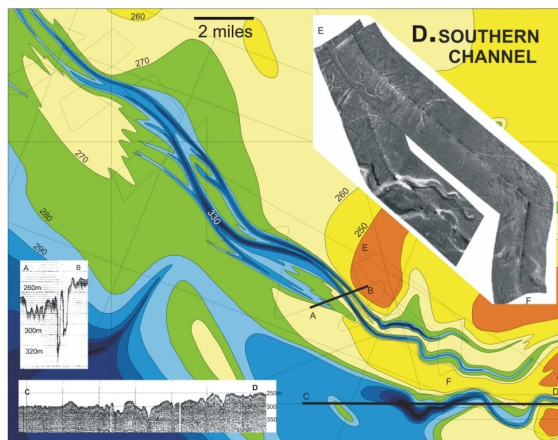
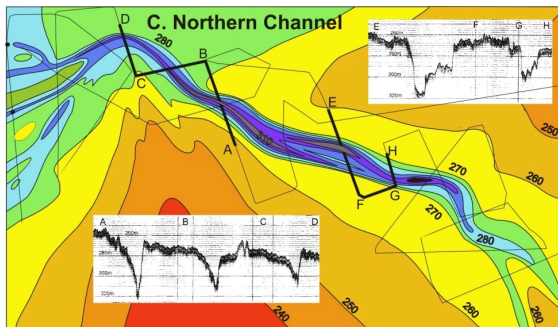


1. Fragment of the IBCAO map (Jakobsson et al., 2012) showing general bathymetry with rounded contours of sea bottom non-characteristic for glaciated shelves.
2. Fragment of navigation map with a 200-m isobath and depth readings.
3. Detailed bathymetry constructed in this study using numerous depth readings from navigation map and measurements from continuous seismic records. The resultant bathymetry shows linear pattern characteristic to glacial shelves.
4. Thickness map of SSU-III constructed using the continuous seismic records and detailed bathymetry. Based on the distribution of glacial deposits, we interpret the elongated features as drumlins and the ice flow direction from the northeast.

A. Comparison of the bathymetry charts constructed using different approaches (1-3), and the interpretation of ice dynamics based on the detailed bathymetry and subbottom profiles (4). See Maps 1 and 2 for location of Area A.



B. Comparison of the bathymetry charts (1 and 3) constructed using different approaches, and thickness maps (2 and 4) using different bathymetry. See maps 1 and 2 for location of Area B.



Examples of bathymetry and subbottom profiles of seafloor channels (to 60 m deep) crossing the Admiralty Bank moraines. We infer that these channels were the main pathways for sediment constructing the ATB in the Central Deep to the southwest.

C and D. Examples of seafloor channels (to 60 m deep) crossing the Admiralty Bank moraines. We infer that these channels were the main pathways for sediment constructing the ATB in the Central Deep. See maps 1 and 2 for Areas C and D.

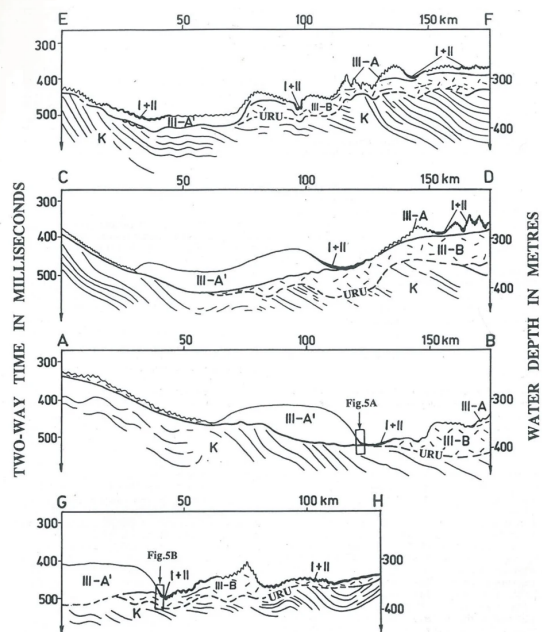


Fig. 3. Cross-section along the regional sparker profiles (see Fig. 2). Seismostratigraphic units are interpreted as: K - Cretaceous bedrock; III-B - basal till; III-A - iceberg-turbated till; III-A' - waterlain till ('transparent body'); I+II - distal glaciomarine and marine deposits. URU - Upper Regional Unconformity.

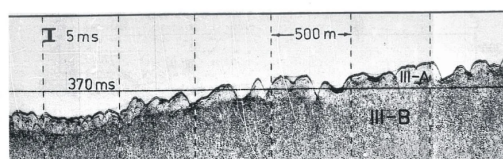


Fig. 4. Sparker record illustrating the structure of the upper part of the seismostratigraphic unit III (Fig. 2A for location).

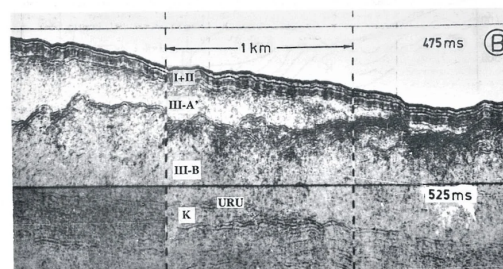
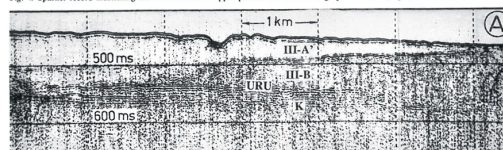
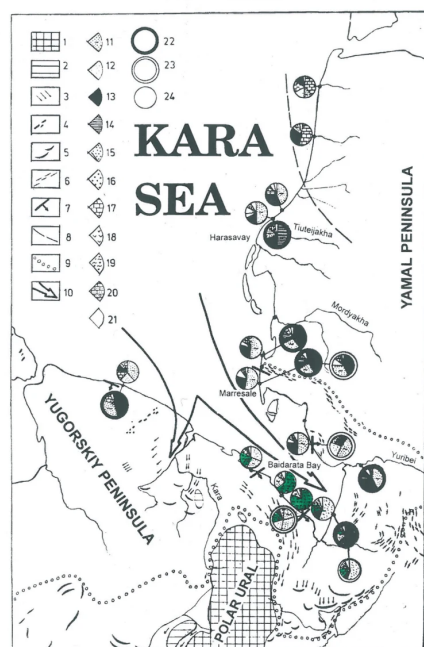
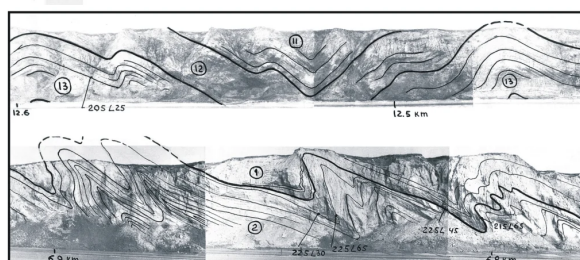


Fig. 5. Sparker records illustrating the structure of the 'transparent body' wedging zone. Fig. 5A is a fragment of regional profile C-D, while Fig. 5B is located slightly southwards of profile G-H (Figs. 2 and 3 for location). Seismostratigraphic units are explained in the text and in Fig. 3.

E. and 2. Seismic profiles showing the structure of the ATB (herein SSU-III-A') in the Central Deep (Gataullin et al., 1993). See maps 1 and 2 for Area E.



EVIDENCES FOR GLACIAL DRIFT FROM THE KARA SEA SHELF

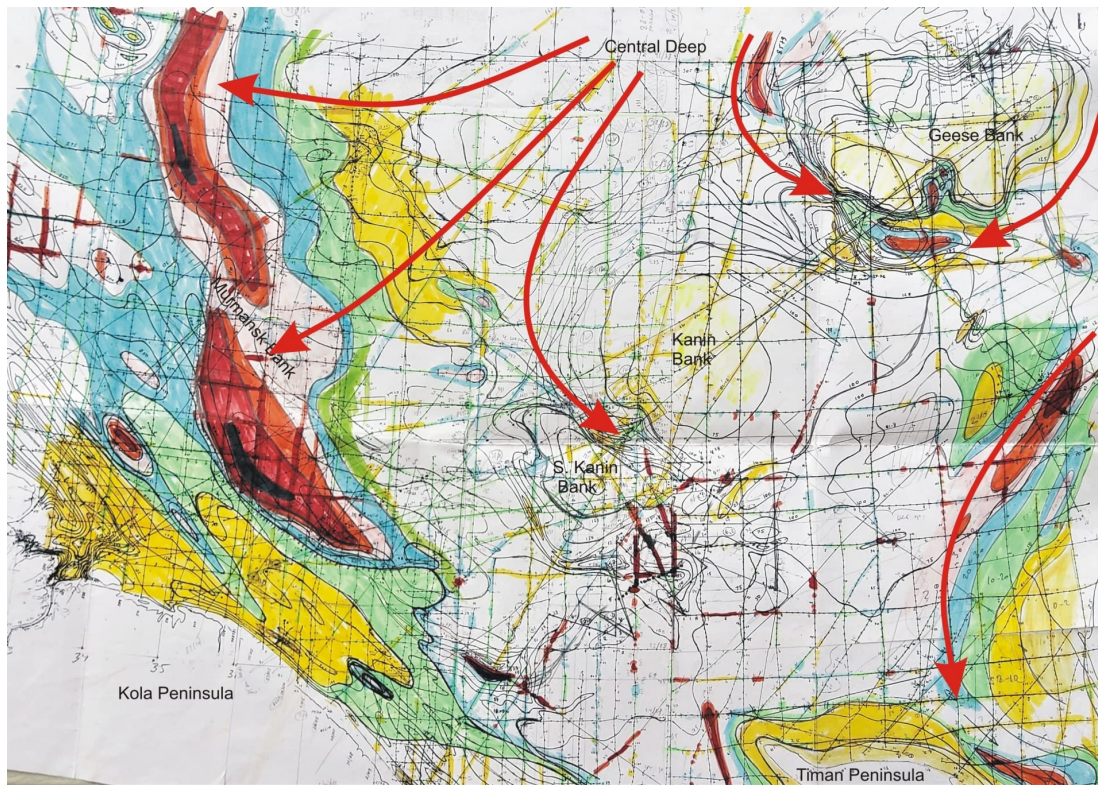


FRAGMENTS OF MARRSACLE CLIFF PHOTOMOSAICS

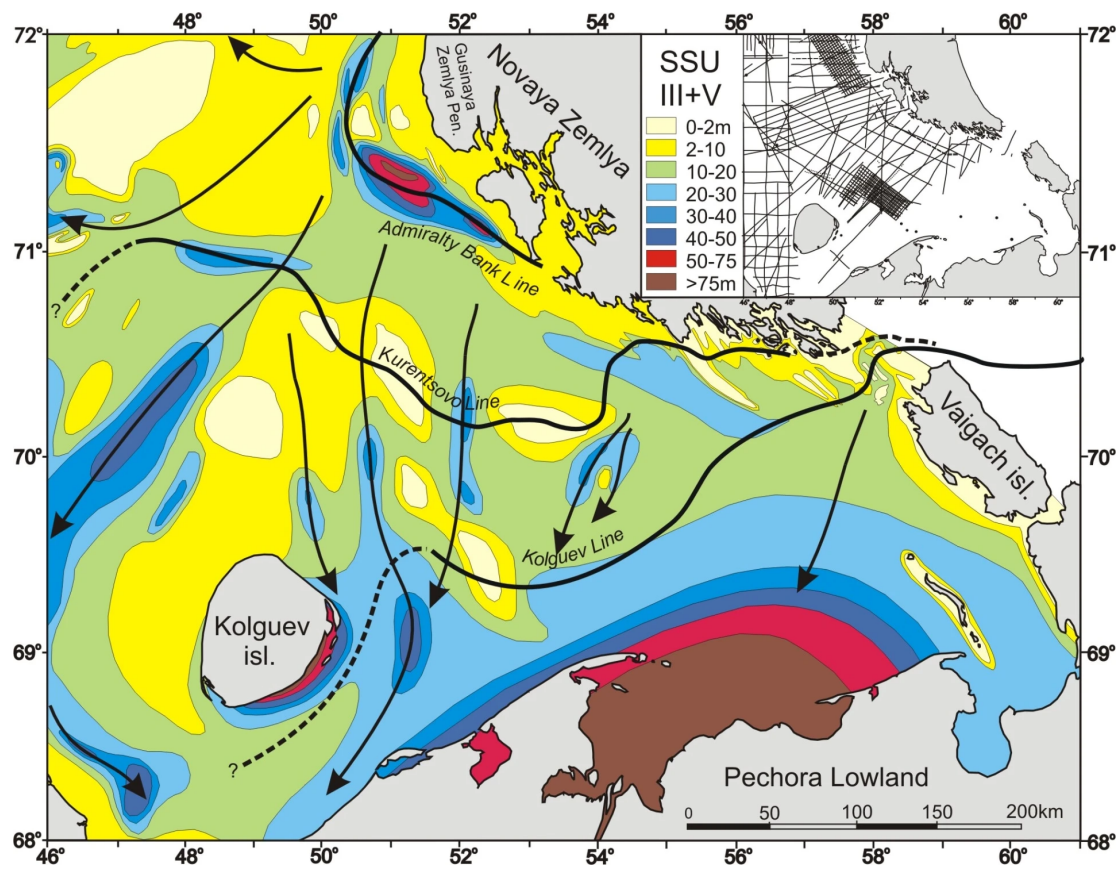
The upper fragment (central zone of 'anticlinorium') shows only simple gentle folds of lower part of the Marresale Formation.
The lower fragment (close to the Kara Till) shows the prevalence of asymmetric folds overturned to N-E.

Glaciotectonic deformations on the western coast of the Yamal peninsula formed by the Baidarata ice lobe moving from the Kara Sea along the Novaya Zemlya Trough.

1. Evidence for pre-LGM glacial advance to the Yamal Peninsula from the Kara Sea shelf (Gataullin, 1988). The occurrence of specific quartz-chlorite shales on the beaches of the Baidarata Bay north the Polar mountains, and their complete absence in the Kara Till on the Yamal Peninsula, contradicts reconstructions (e.g. Forman, et al., 2002) implying ice advance from the Polar Ural.



3. Draft of the SSU-III thickness map, for the SW Barents Sea (Gataullin, 1993). A most prominent sea floor geomorphic feature in this area is the Murmansk bank, which we interpreted as a morainic ridge. Other researches (e.g., Bjarnadottir et al., 2014) suggest it as a grounding zone wedge (GZW) deposited at the margin of streaming ice. The overall geomorphic and depositional pattern indicates to glacial stillstand during ice retreat and general glacial advance from the NE. This ice-dynamic pattern does not support the ice divide proposed for the central Barents Sea (Andreassen et al., 2013; Esteves, et al., 2017).



4. Thickness map of glacial till (combined SSU-III and V) in the Pechora Sea (southeasternmost Barents Sea), showing the general ice-flow direction from the north, the LGM limit (Kolguev line), and two ice stillstands during deglaciation: Kurentsovo line and Admiralty Bank line (Gataullin et al., 2001).

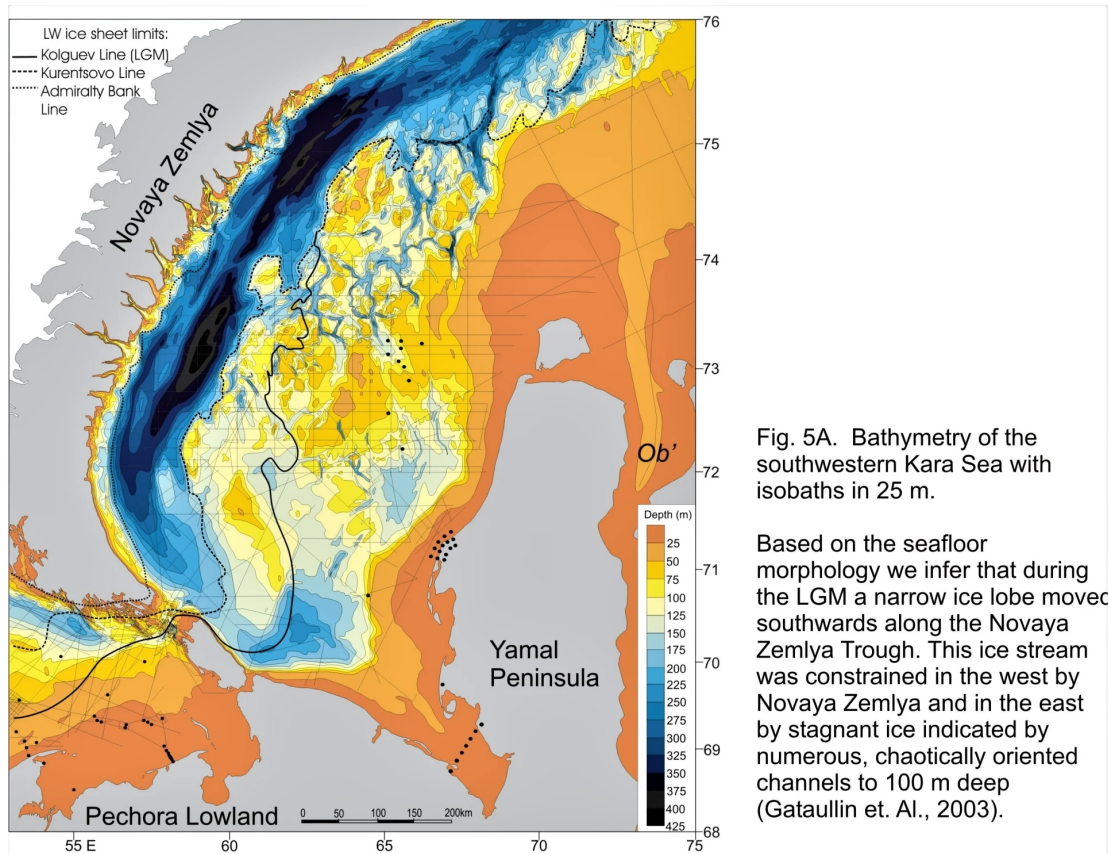


Fig. 5A. Bathymetry of the southwestern Kara Sea with isobaths in 25 m.

Based on the seafloor morphology we infer that during the LGM a narrow ice lobe moved southwards along the Novaya Zemlya Trough. This ice stream was constrained in the west by Novaya Zemlya and in the east by stagnant ice indicated by numerous, chaotically oriented channels to 100 m deep (Gataullin et al., 2003).

5A. Bathymetry of the southwestern Kara Sea.

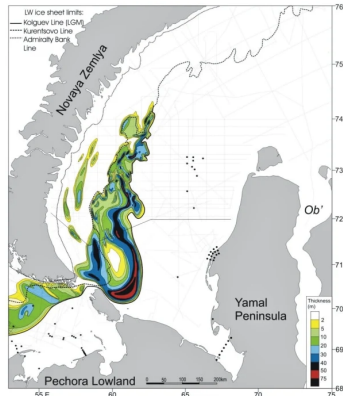


Fig. 7. Isopach map of SSU-IIIa (Late Weichselian Kolguev Till)

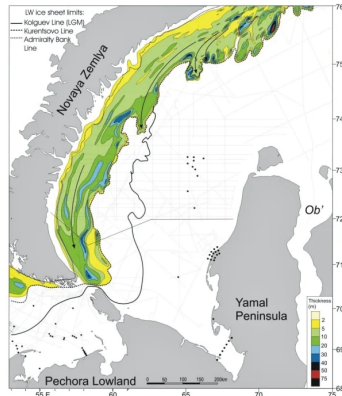


Fig. 8. Isopach map of SSU-IIIb (Late Weichselian Kurentsovo Till)

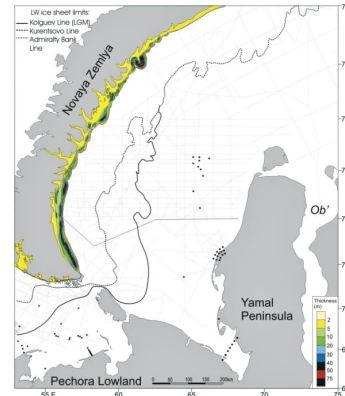
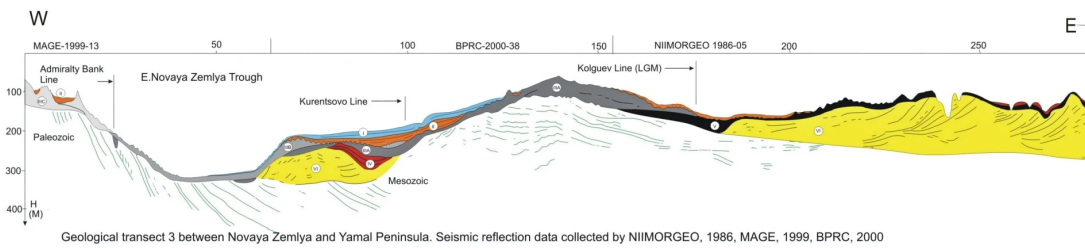
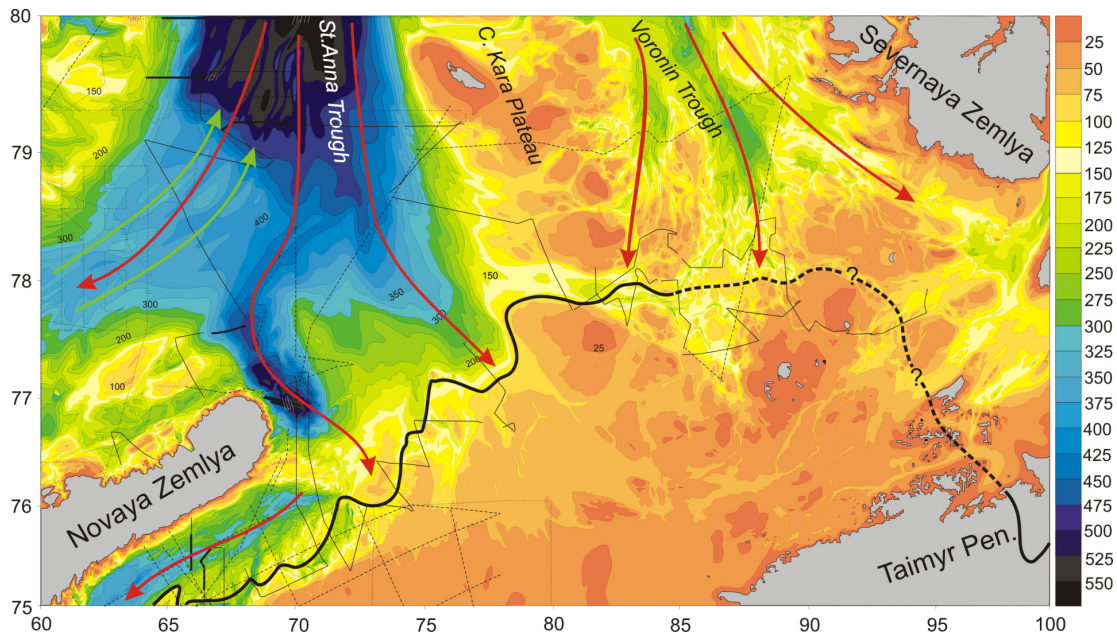


Fig. 9. Isopach map of SSU-IIIc (Late Weichselian Admiralty Bank Till)



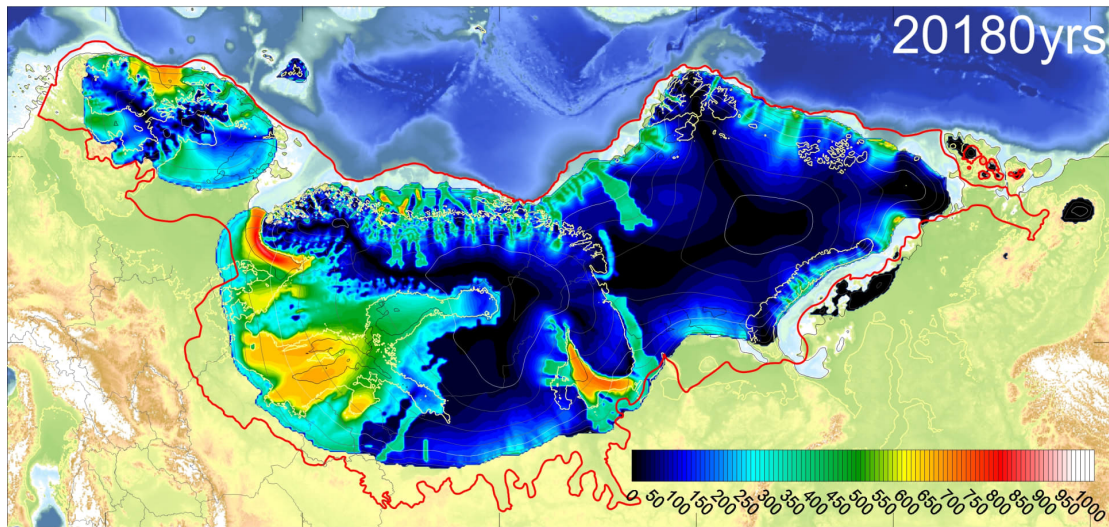
Geological transect 3 between Novaya Zemlya and Yamal Peninsula. Seismic reflection data collected by NIIMORGEO, 1986, MAGE, 1999, BPRC, 2000

5B. Thickness maps of glacial deposits (SSU-III A-C) in the southwestern Kara Sea during the LGM and deglaciation stillstands; and a geological profile between Novaya Zemlya and Yamal Peninsula (Gataullin et al., 2003).



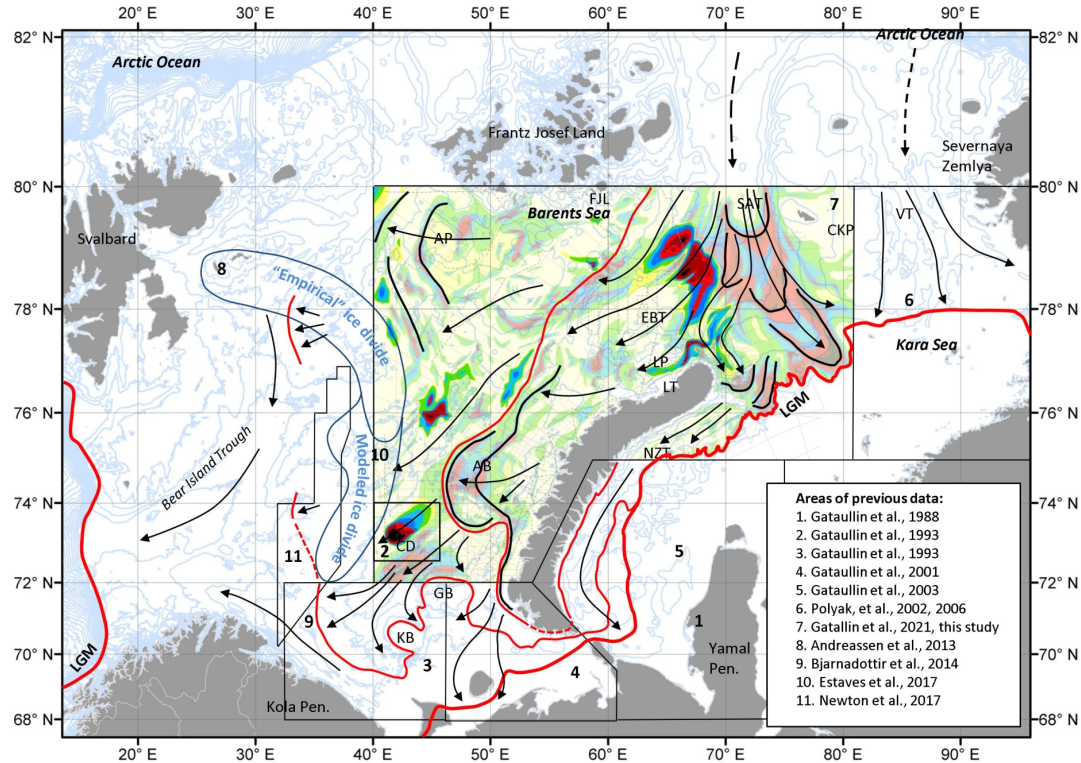
6. Bathymetry of the eastern Barents Sea with isobaths in 25 m (Polyak et al, 2002). North of the LGM limit (black line) sea floor has linear geomorphic features and accumulations of glacial deposits (SSU-III). To the south, sea bottom has rounded morphology with depressions filled by pro- and post-glacial sediments and an alluvial plain further south. This pattern indicates that during the LGM ice invaded the Kara Sea from the north and blocked the northbound drainage of Siberian rivers.

EURASIAN ICE SHEET COMPLEX (EISC) MODEL (PATTON ET AL., 2016)



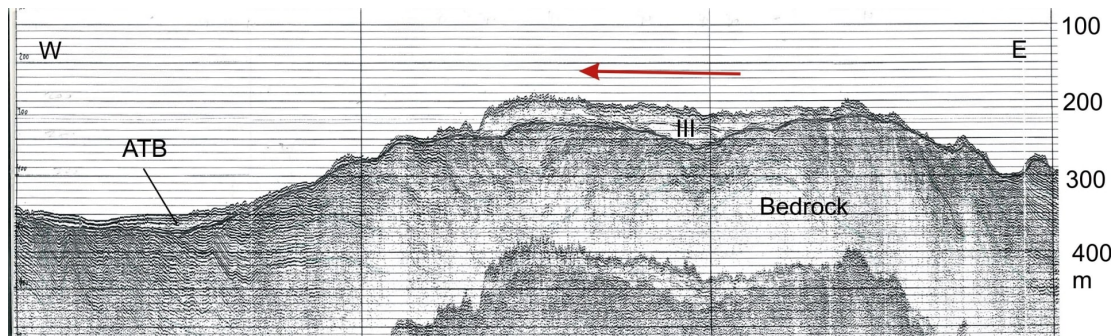
Modeled ice-surface velocity during the Last Glacial Maximum (LGM) (Patton et al., 2016). Data from the eastern Barents and Kara Seas presented here do not support this model for the eastern portion of EISC.

MAP 3. OVERVIEW OF THE BARENTS-KARA ICE SHEET

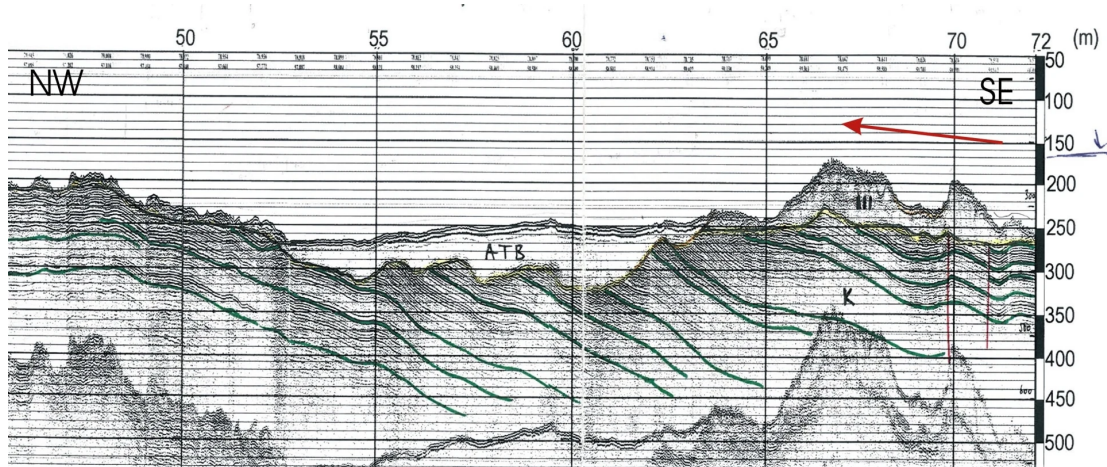


Interpretation of ice dynamics of the Barents - Kara Ice Sheet during the LGM and subsequent deglaciation. See Figs 2 and 3 for explanation of the thickness of glacial sediments. General southward ice movement is inferred from the Arctic Ocean along the Saint Anna and Voronin Troughs. Previously proposed empirical (Andreassen et al., 2013) and modeled (Estaves et al., 2017) ice divides in the central Barents Sea are not supported by the presented data east of this area.

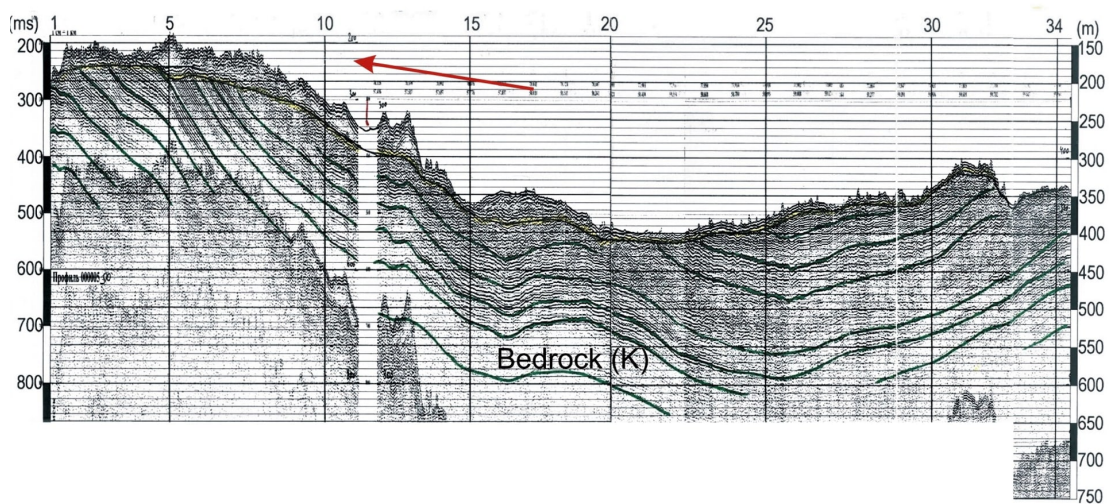
SUPPORTING SEISMO-STRATIGRAPHIC DATA (1-8)



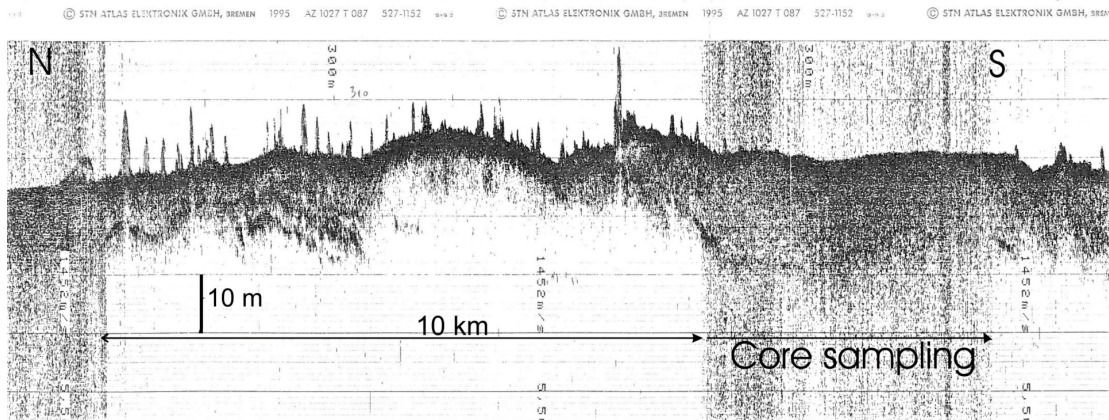
Seismic profile 1 across a morainic ridge and a small ATB indicating a westward re-advance and a brief stillstand during deglaciation.



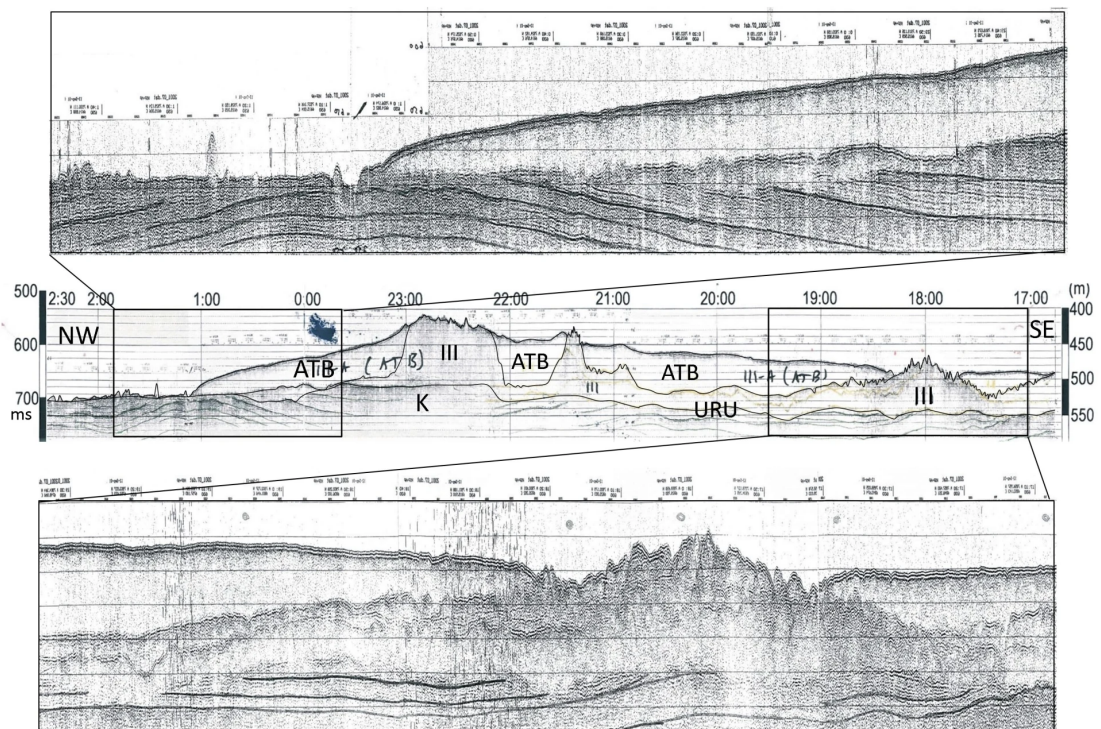
Seismic profile 2. ATB west of morainic ridge indicating ice flow from the east (from the SAT).



Seismic profile 3 shows a morainic ridge formed by glacial re-advance from the east (from the SAT) and spiky sea-floor features indicate glacial lineations at the bottom of the East Barent Trough, likely formed by an ice stream moving towards the SAT during deglaciation.



Profile 4. Fragment of a high resolution Parasound profile showing glacial lineation in the East Barents Trough.



Seismic profile 5 along the western slope of SAT crosses a series of narrow and elongated ridges composed by glacigenic deposits (SSU-III) with chaotic acoustic signature and saw-like surface (possibly large drumlins); ice-proximal deposits with acoustically transparent signature (ATB) are located between the ridges. Spiky seafloor bedforms (up to 15 m high) indicate glacial lineations on the left side of upre profile.

Seismic profile 8 along the southeastern portion of the SAT. Thickening of glaciogenic deposits (SSU-III) to more than 75 m indicates glacial advance southwards from the SAT. The LGM till is underlain by a possibly interglacial layer (SSU-IV) and remnant of an older Kara Till (SSU-V).

Notice!

Your iPoster has now been unpublished and will not be displayed on the iPoster Gallery.

You need to publish it again if you want to be displayed.

AUTHOR INFORMATION

Valery Gatallin, Lehman College, City University of New York, NY, USA, gataull@msn.com

Yuri Gorokhovich, Lehman College, City University of New York, NY, USA, yuri.gorokhovich@lehman.cuny.edu

Leonid Polyak, Byrd Polar Research and Climate Center, Ohio State University, Columbus, OH, USA, polyak.1@osu.edu

ABSTRACT

Our knowledge of glacial history of the western (Norwegian) part of the Barents Sea has greatly improved during the last decades, notably due to the high-resolution multibeam swath bathymetry data. In contrast, published seafloor data from the eastern part of the Barents Sea and the Kara Sea are much more sparse. This study presents new geophysical/geological evidence for reconstructing glacial dynamics of the eastern part of the Barents-Kara Ice Sheet during the Last Glacial Maximum and subsequent deglaciation.

Archival data used in this study include more than 300,000 km of sparker and high-resolution Parasound profiles verified by boreholes drilled with continuous core recovery to 50-100 m below sea bed. This dataset was used to construct continuous geological cross-sections and a series of maps, including detailed bathymetry (in 10-m isobaths) and sediment thickness maps of major seismo-stratigraphic units. Based on the bathymetric and sediment thickness data we map megascale glacial lineations, drumlin-like ridges up to 50 m high and subglacial channels up to 100 m deep, as well as accumulations of glacial deposits (basal, lateral and end moraines) and ice-proximal acoustically transparent bodies (ATBs).

Spatial and stratigraphic analysis of these bedforms enables us to put forward a new hypothesis that ice moved on the shelf from the Arctic Ocean along the Saint Anna Trough (SAT). Further south, near the northern tip of the Novaya Zemlya islands, the ice flow split into three major lobes moving to the southwest into the Barents Sea and to the south and southeast into the Kara Sea. Deglaciation in the study area progressed with several ice stillstands and subsequent readvances marked by end-moraines and accumulation of ice-proximal sediments. During deglaciation events, when the SAT became ice free due to iceberg calving, the ice flow reversed its direction toward the SAT, forming a fluting and a massive ATB on the western SAT slope. The exact timing and mechanisms of the ice transgression(s) from the Arctic Ocean are not well understood. Additional high-resolution data such as multibeam bathymetry surveys are needed to verify the spatiotemporal distribution of glaciogenic bedforms, and glaciological modeling is required to comprehend the ice dynamics and put it in the pan-Arctic context.

REFERENCES

Reference:

1. Gataullin, V., 1988. Upper Quaternary deposits of the western coast of Yamal Peninsula. Ph.D. Thesis, Leningrad, Russia.
2. Gataullin, V., Polyak, L., Epshtein, O., Romanyuk, B., 1993. Glacigenic deposits of the Central Deep: a key to the Late Quaternary evolution of the eastern Barents Sea. *Boreas* 22, 47-58.
3. Gataullin, V., et al., 1993. Lithostratigraphic investigations of the key geotechnical boreholes of the Barents and Kara Sea. Technical Report, NIIMorgeo, Riga, Latvia, 363 pp. (in Russian).
4. Gataullin, V., Mangerud, J., Svendsen, J.I., 2001. The extent of the Late Weichselian ice sheet in the southeastern Barents Sea. *Global and Planetary Change* 31, 453-474.
5. Gataullin, V., Polyak, L., Belyaev, V., Gainanov, V., Sang, S., 2003. Late Pleistocene glaciation history of the southwestern Kara Sea. XVI INQUA Congress, Program with Abstracts. pp. 71-72, Reno, NV: Desert Research Institute.
6. Polyak, L., Gataullin, V., Gainanov, V., Gladyshev, V., Goremykin, Y., 2002. Kara Sea expedition yields insight into extent of LGM ice sheet. *EOS. Transactions of the American Geophysical Union* 83, 525, 529.
7. Gataullin, V., Gorokhov, Y., Polyak, L., 2021. New sea floor evidence of glacial dynamics of the Barents-Kara Ice Sheet during LGM suggests glacial advance from the Arctic Ocean. This presentation.
8. Andreassen, K., Winsborrow, M., Bjarnadottir, L., Ruther, D., 2014. Ice stream retreat dynamics inferred from an assemblage of landforms in the northern Barents Sea. *Quaternary Science Reviews* 92, 246-257.
9. Bjarnadottir, L., Winsborrow, M., Andreassen, K., 2014. Deglaciation of the central Barents Sea. *Quaternary Science Reviews* 92, 208-226.
10. Esteves, M., Bjarnadottir, L., Winsborrow, M., Chakleton, C., Andreassen, K., 2017. Retreat patterns and dynamics of the Sentralbankrenna glacial system, central Barents Sea. *Quaternary Science Reviews* 169, 131-147.
11. Newton, A., Huuse, M., 2017. Glacial geomorphology of the central Barents Sea: Implications for the dynamic deglaciation of the Barents Sea Ice Sheet. *Marine Geology* 387, 114-131.
12. Forman, S., Ingolfsson, O., Gataullin, V., Manley, W., Lokrantz, H., 2002. Late Quaternary Stratigraphy, Glacial Limits, and Paleoenvironments of the Marresale Area, Western Yamal Peninsula, Russia. *Quaternary Research*, 57, 353-370.
13. Jacobsson, M., et al., 2012. The International Bathymetric Chart of the Arctic Ocean (IBCAO) version 3.0, *Geophys. Res. Lett.* 39.
14. Patton, H., Hubbard, A., Andreassen, K., Winsborrow, M., Stroeve, A., 2016. The Build-up, configuration, and dynamical sensitivity of the Eurasian ice-sheet complex to Late Weichselian climatic and oceanic forcing. *Quaternary Science Reviews*, 153, 97-121.

Acknowledgement:

This work was performed thanks to grants from US National Science Foundation awards OPP-9818247 and OPP-0221468 to Leonid Polyak and a contract from the Center for Arctic Gas Hydrate, Environment and Climate (GAGE), University of Tromsø, Norway.